JACS
JOURNAL OF THE AMERICAN CHEMICAL SOCIETY
Cite This: J. Am. Chem. Soc. 2019, 141, 4526−4530
Communication
pubs.acs.org/JACS

Designing a Green Fluorogenic Protease Reporter by Flipping a Beta Strand of GFP for Imaging Apoptosis in Animals

Qiang Zhang,[¶,§] Antonino Schepis,[§,‡] Hai Huang,[§,‡] Junjiao Yang,[¶,§,‡] Wen Ma,[∥,‡] Joaquim Torra,[¶,§,†] Shao-Qing Zhang,[⊥] Lina Yang,[#] Haifan Wu,[¶,§] Santi Nonell,[†] Zhiqiang Dong,[#] Thomas B. Kornberg,[§] Shaun R. Coughlin,[§] and Xiaokun Shu*[,¶,§]

[¶]Department of Pharmaceutical Chemistry, University of California−San Francisco, San Francisco, California 94158, United States
[§]Cardiovascular Research Institute, University of California−San Francisco, San Francisco, California 94158, United States
[∥]Department of Chemistry and Biochemistry, University of California San Diego, La Jolla, California 92093, United States
[†]Institut Químic de Sarrià, Universitat Ramon Llull, Via Augusta 390, 08017 Barcelona, Spain
[⊥]Department of Neurology, Harvard Medical School and MassGeneral Institute for Neurodegenerative Disease, Massachusetts General Hospital, Charlestown, Massachusetts 02129, United States
[#]Bio-Medical Center, College of Life Science and Technology, Huazhong Agricultural University, Wuhan, Hubei 430070, China

Supporting Information

ABSTRACT: A family of proteases called caspases mediate apoptosis signaling in animals. We report a GFP-based fluorogenic protease reporter, dubbed "FlipGFP", by flipping a beta strand of the GFP. Upon protease activation and cleavage, the beta strand is restored, leading to reconstitution of the GFP and fluorescence. FlipGFP-based TEV protease reporter achieves 100-fold fluorescence change. A FlipGFP-based executioner caspase reporter visualized apoptosis in live zebrafish embryos with spatiotemporal resolution. FlipGFP also visualized apoptotic cells in the midgut of *Drosophila*. Thus, the FlipGFP-based caspase reporter will be useful for monitoring apoptosis during animal development and for designing reporters of proteases beyond caspases. The design strategy can be further applied to a red fluorescent protein for engineering a red fluorogenic protease reporter.

Proteases play fundamental roles in many signaling pathways. One family of protease, caspase, executes cell apoptosis. The apoptosis signaling pathway is composed of extrinsic and intrinsic pathways that are activated by stimuli such as DNA damage, oncogenes, and developmental cues.[1,2] Both pathways lead to activation of the executioner caspases that cleave thousands of substrates, resulting in cell apoptosis.[3] Activity reporters of executioner caspases thus visualize apoptosis signaling. Furthermore, mechanistic understanding of cell and developmental biology requires investigation of cell signaling in living animals. To image spatiotemporal dynamics of apoptosis in animals especially developing animals, it is ideal to use genetically encoded fluorescent protease reporters. However, fluorescence imaging of living animals is challenging because of tissue autofluorescence, cell heterogeneity and rapid shape and position changes. Thus, to enable in vivo imaging, protease reporters should have large dynamic range (i.e., large fluorescence increase upon protease activation) and high brightness (i.e., high quantum yield). Over the past few years, to overcome limitations of FRET-based executioner caspase reporters,[4−7] many different types of reporters have been developed.[8−13] For example, the bipartite GFP was previously engineered into a light-driven protease sensor.[11] Here we report a new type of rationally designed fluorogenic protease reporter based on GFP with both large dynamic range and high brightness. And we demonstrate its application in imaging apoptosis in zebrafish embryos.

To design a GFP-based fluorogenic protease reporter with large dynamic range, we modified the self-assembling split GFP so that its self-assembly is regulated by protease activity. GFP contains 11 beta strands (β-strands) and a central α-helix (Movie S1),[14,15] which can be split into three parts. One part contains nine β-strands and the central α-helix (β1−9); a second part contains 10th β strand (β10); and the third part contains 11th β strand (β11).[16] β1−9 contains three amino acids that form the chromophore;[17,18] whereas β11 contains the highly conserved Glu222 that catalyzes chromophore maturation.[19] It has been shown that when β10 and β11 are linked together or are in close proximity, they rapidly bind to β1−9, and green fluorescence develops within several tens of minutes.[20] This has been used to detect protein−protein interactions,[20] including interaction between G protein coupled receptor (GPCR) and beta-arrestin upon activation and phosphorylation of GPCR.[21]

GFP structure suggests a compact fit of β1−9 and β10−11 (Figure 1a), which presumably provides structural basis of high binding affinity between them (Movie S2). On this basis, we sought to prevent β10−11 binding to β1−9 until protease activation. To achieve this, we redesigned β10−11. GFP structure shows that β10−11 forms an antiparallel β-strands, which fit well with the rest of the structure (Figure 1a). We hypothesized that if β10−11 was redesigned so that it forms a parallel structure, then it would no longer fit β1−9. To flip

Received: December 12, 2018
Published: March 1, 2019

DOI: 10.1021/jacs.8b13042
J. Am. Chem. Soc. 2019, 141, 4526−4530

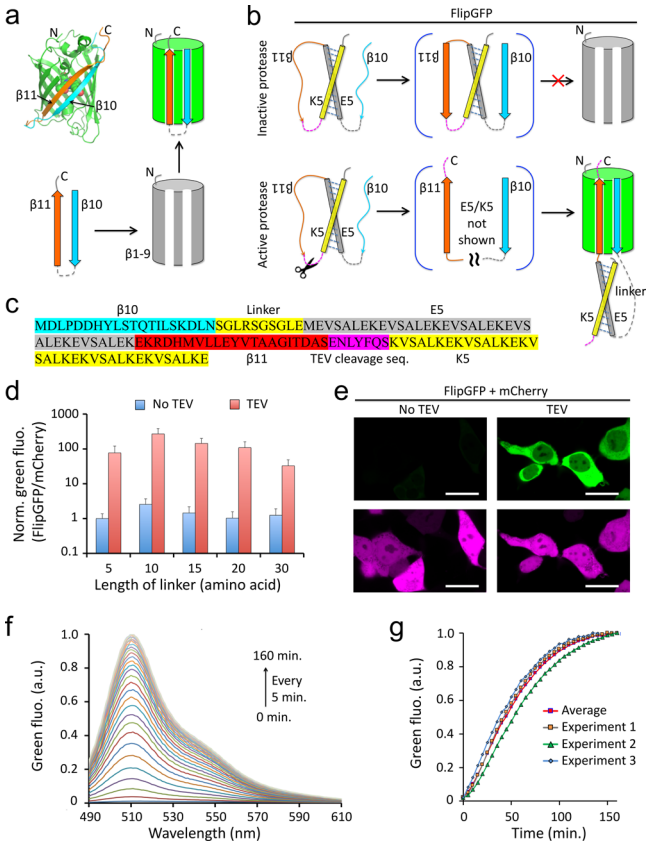

Figure 1. Rational design of a green fluorogenic protease reporter FlipGFP. (a) Schematic. (b) FlipGFP. (c) Sequence. (d) Normalized fluorescence (HEK293). The error bars represent standard deviation (n = 3). (e) Fluorescence images. (f) Representative emission spectra of FlipGFP over time. FlipGFP (β1−9 and the cleaved β10−11) were purified and mixed (β1−9:2.9 μM; β10−11:6.5 μM). (g) Fluorescence intensity (integrated from 490 to 550 nm) over time after mixing β1−9 and cleaved β10−11. Scale bars, 20 μm.

β11, we utilized heterodimerizing coiled coils E5 and K5: we linked β10/β11 with E5; β11 was followed by K5; the protease cleavage sequence was inserted between β11 and K5 (Figure 1b, c).

Based on this design, E5/K5 heterodimer "flips" β11 and prevents self-assembly of the split GFP (Figure 1b, Figure S1). Upon protease cleavage, β11 flips back, forming an antiparallel structure with β10, which enables self-assembly with β1−9 and leads to fluorescence increase. We named this reporter FlipGFP. As a proof of concept, we designed a TEV protease reporter by inserting TEV cleavage sequence into FlipGFP, which achieved 77-fold fluorescence increase upon TEV cleavage in HEK293 cells (Figure 1d, linker length = 5 amino acids).

Because efficient assembly between cleaved β10−E5−β11 and β1−9 is likely dependent on distance between β10 and E5 (Figure 1b), we increased length of the linker between β10 and E5 from 5 amino acid (aa) to 10, 15, 20, 30 aa. Characterization of the FlipGFP variants in HEK293 cells indicated that the FlipGFP with 10aa linker showed the largest fluorescence increase (106-fold) upon TEV cleavage and the highest brightness (Figure 1d,e). On the other hand, when the linker was 30aa, the fluorescence increase was narrowed to 26-fold. Interestingly, in the inactive state (i.e., no TEV protease), this FlipGFP with 30aa linker was as dim as the FlipGFP with 5aa linker. But in the active state (i.e., cleaved by TEV protease), the FlipGFP with 30aa linker was much dimmer than the FlipGFP with 5aa linker. This suggests that while elongation of the linker length from 5aa to 10aa increases the assembly efficiency of the split GFP, further elongation of the linker to 30aa decreases reconstitution efficiency. We thus decided to use 10aa linker length for FlipGFP from now on. Fluorescence quantum yield of reassembled FlipGFP was determined to be 0.66 ± 0.03.

We next measured kinetics of FlipGFP-based protease reporter to determine its temporal resolution. First, we separately purified two parts of FlipGFP in the presence of TEV protease. Then we mixed the cleaved FlipGFP and monitored green fluorescence over time. The green fluorescence increased over time with time to half-maximal fluorescence ($T_{1/2}$) of 43 ± 6 min (Figure 1f,g), which is similar to the previously reported kinetics of the split GFP self-assembly.[16,20] The proposed working mechanism of FlipGFP was supported by circular dichroism spectroscopy and molecular dynamics simulation (Figures S1−3, Movies S3−4, SI). Lastly, to obtain large fluorescence change, the expression level of FlipGFP needs to be titrated in cells (Figure S4).

To design a FlipGFP-based caspase reporter for imaging apoptosis, we replaced the TEV cleavage sequence with the consensus cleavage sequence (DEVD) of caspase-3 in FlipGFP (Figure 2a). The well characterized signaling pathways of apoptosis are composed of extrinsic and intrinsic pathways, both of which lead to activation of the executioner caspases that include caspase-3.[3] And the conserved cleavage sequence (DEVD) of caspase-3 has been used in the previous caspase reporters.[7,9,10,12,22,23]

We expressed FlipGFP in the HeLa cells. Upon addition of staurosporine, which induces apoptosis by activating caspase 3,[24] FlipGFP's green fluorescence increased significantly in cells treated with staurosporine (Figure 2b, Movie S5), whereas the fluorescence signal of FlipGFP has no or little change in cells without treatment with staurosporine (Movie S6). And the onset of apoptosis in single cells as detected by FlipGFP varied around 2 to 5 h after addition of staurosporine (Figure 2c, Movies S7−8, Figure S5), consistent with previous results.[25] Activation of caspase-3 in FlipGFP fluorescing cells was confirmed using a commercially available small molecule active-site modifier for far-red fluorescent imaging of caspase-3 activity (Figure 2d).

To determine whether the fluorescence signal and the temporal resolution of FlipGFP are sufficient for imaging apoptosis in animals, we expressed the FlipGFP-based caspase reporter in zebrafish. Zebrafish was chosen based on optical transparency and its importance as a model organism among vertebrate animals.[26] To demonstrate that FlipGFP could be used to visualize spatiotemporal dynamics of apoptosis during embryo development, we injected mRNA encoding two parts of FlipGFP caspase reporter linked with a T2A site and mCherry into the embryo at the one-cell stage. T2A is a "self-cleaving" peptide used in coexpression of multiple genes.[27]

Time-lapse imaging of the head was started at 24 h postfertilization (hpf) (Figure 2e). At this time, little green fluorescence was observed (Figure 2e, Movie S9). Ten hours later, green fluorescence was detected in a couple of cells. After 15−20 h, more cells showed strong green fluorescence. By contrast, mCherry fluorescence was weak and decreased over time, presumably because its mRNA injected at the one-cell stage was degraded over time and/or diluted as development

DOI: 10.1021/jacs.8b13042
J. Am. Chem. Soc. 2019, 141, 4526−4530

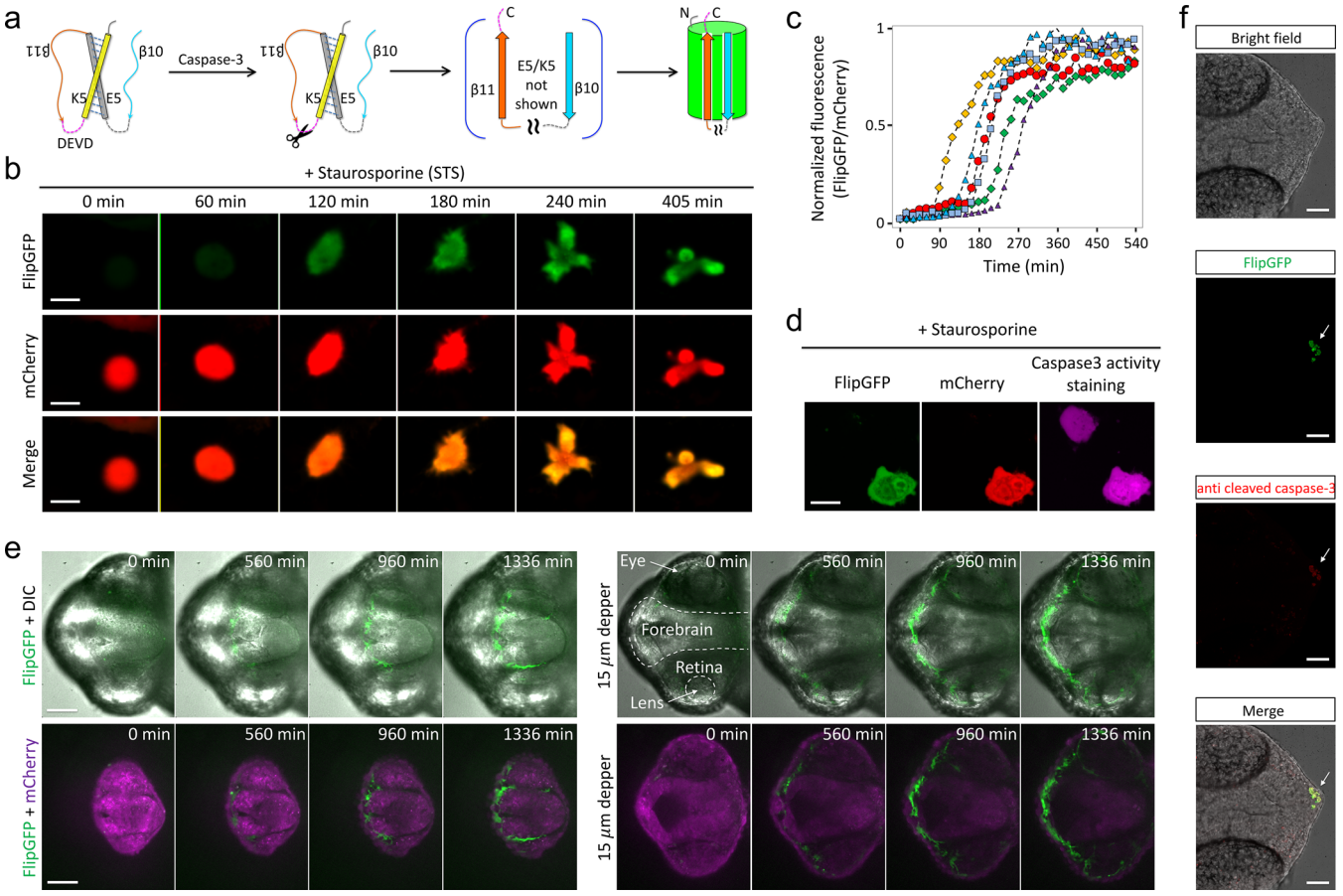

Figure 2. FlipGFP-based caspase reporter in imaging apoptosis in mammalian cells and in zebrafish. (a) Schematic. (b) Fluorescence images of HeLa cells upon addition of staurosporine (Movie S5). (c) Representative cells (Figure S5). (d) FLICA staining. (e) Time-lapse images of zebrafish embryo expressing FlipGFP (green), mCherry (purple). Imaging started at 24 hpf (Movie S9). (f) Whole mount immunostaining of zebrafish embryo expressing FlipGFP. Arrow points to apoptotic cells. Embryos were fixed with 4% PFA at 27 hpf. Scale bars: 20 μm (b, d); 70 μm (e); 50 μm (f).

progressed. Green, presumed apoptotic cells were distributed around the developing forebrain and the retina. In particular, time-lapse imaging first detected green fluorescence on the rostral aspect of the forebrain. The number of green cells increased over time and they appeared to form clusters. These cells appeared to have neuron-like long extensions or processes (Figure 2e). We also imaged at 15 μm deeper layer of the brain, which revealed similar distribution of the apoptotic cells (Figure 2e, right). Furthermore, z-section imaging indicated that many of them appeared to be located on the outer layer of the forebrain and the retina (Movie S10). The activity of caspase-3 was confirmed using antibody staining against cleaved caspase-3 (Figure 2f, Figure S6). The spatial pattern of FlipGFP fluorescence we observed is consistent with a previous study based on TUNEL staining that showed apoptotic cells in the developing brain.[28]

After demonstration of FlipGFP in zebrafish, we decided to show whether it can also be used in detecting apoptosis in another important model organism *Drosophila*. Because of the genetic tractability and plethora of available genetic tools, *Drosophila melanogaster* is an attractive model organism in developmental biology. To demonstrate FlipGFP-based caspase reporter in imaging apoptosis in this model organism, we first created a transgenic UAS-FlipGFP *Drosophila*.

In the midgut of adult *Drosophila*, enterocytes are the largest class of differentiated intestinal cells.[29,30] At physiological condition, a small number of enterocytes are believed to undergo apoptosis that is caused by passage, digestion and absorption of food and various xenobiotics.[30−32] However, detection of this low level of physiological apoptosis has been difficult, presumably due to lack of a sensitive and robust method. To express FlipGFP in the enterocytes of the midgut, we crossed UAS-FlipGFP with Myo1A-GAL4. To mark all of the enterocytes, we coexpressed the red fluorescent protein mCherry. Fluorescence imaging of the midgut of the adult fly revealed a couple of enterocytes that were green fluorescent while most enterocytes were not, though they were all red fluorescent from mCherry (Figure 3a). This data suggests that FlipGFP is able to visualize physiological apoptosis in the midgut. Furthermore, we confirmed that green fluorescent cells were apoptotic cells using antibody staining against cleaved caspase-3 (Figure 3b). Additionally, we also showed that FlipGFP imaged apoptosis in the eye disc of *Drosophila* (Figure S7). Our data demonstrates that FlipGFP-based caspase reporter can visualize apoptotic cells and will thus be a valuable tool for investigating apoptosis in *Drosophila*.

Lastly, we attempted to design a red fluorogenic protease reporter based on the same approach. Initially, the protease reporter based on the super folder Cherry (sfCherry) failed to fluoresce in HEK293 cells (Figure S8),[33] presumably due to its inefficient self-assembly. On the other hand, after seven rounds of directed evolution of sfCherry (Figure 4a, b) and three

DOI: 10.1021/jacs.8b13042
J. Am. Chem. Soc. 2019, 141, 4526−4530

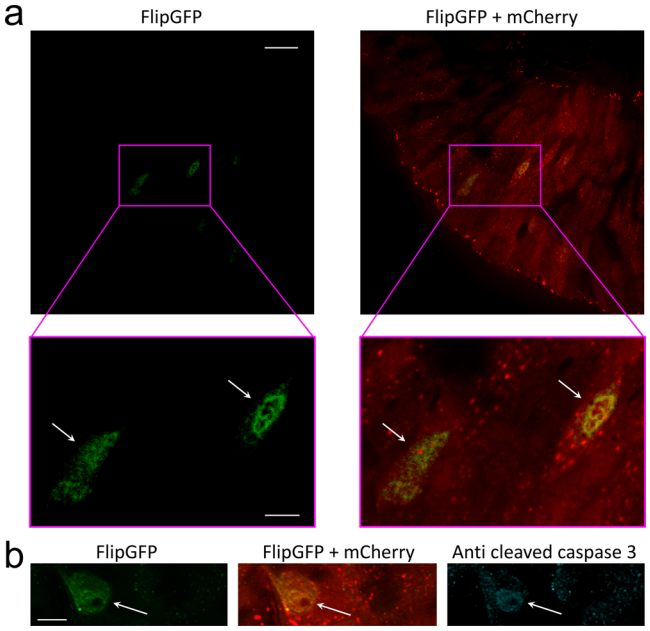

Figure 3. FlipGFP caspase reporter in imaging apoptosis in Drosophila. (a) Confocal images of FlipGFP in the midgut of *Drosophila*. FlipGFP was expressed in enterocytes by crossing UAS-FlipGFP with Myo1A-GAL4. mCherry was expressed. (b) Antibody staining against cleaved caspase 3 (and thus active caspase 3). Arrows point to apoptotic cells. Scale bars: 30 μm (a, top); 10 μm (a, bottom); 10 μm (b).

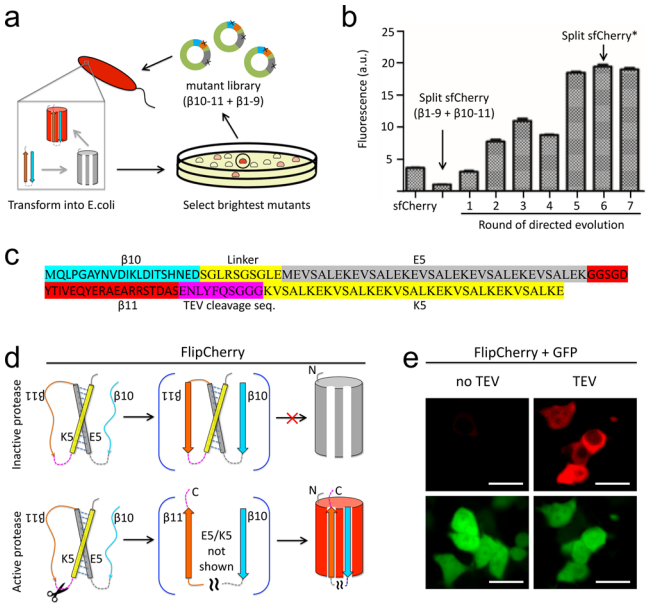

Figure 4. Engineering a red fluorogenic protease reporter FlipCherry. (a) Schematic. (b) Improved split sfCherry* (SI). (c) Sequence of "flipped" β10−11 of engineered split sfCherry*. (d) Schematic showing FlipCherry. (e) Fluorescence images of HEK293 cells. The fold of fluorescence change of FlipCherry upon TEV cleavage was 22 ± 4 (standard deviation, n = 3). Scale bar, 30 μm.

rounds of optimization of the "flipped" β10−11 (Figures S8−9, Table S1), we eventually obtained a red fluorogenic protease reporter: it was not red fluorescent in the absence of TEV protease; but it became red fluorescent (22-fold) when TEV protease was coexpressed in HEK293 cells (Figure 4c−e).

In summary, we have designed a new approach, i.e. "flipping" a beta strand of GFP, in developing GFP-based fluorogenic protease reporters. FlipGFP-based protease reporter achieves ~100-fold fluorescence increase upon proteolytic cleavage, which greatly facilitates imaging of protease activity *in vivo*.[34,35] This approach can be applied to GFP-like other color fluorescent proteins, and multicolor protease reporters will enable simultaneous imaging of multiple protease activities in living cells and animals.[36]

■ ASSOCIATED CONTENT

Supporting Information

The Supporting Information is available free of charge on the ACS Publications website at DOI: 10.1021/jacs.8b13042.

Movies S1−10 (ZIP)

DNA constructs, protein purification and characterization, imaging, characterization of FlipGFP, engineering a red fluorogenic protease reporter (PDF)

■ AUTHOR INFORMATION

Corresponding Author

*xiaokun.shu@ucsf.edu

ORCID

Haifan Wu: 0000-0002-2050-9950

Santi Nonell: 0000-0002-8900-5291

Xiaokun Shu: 0000-0001-9248-7095

Author Contributions

‡These authors contributed equally.

Funding

This work was supported by National Institute of General Medical Sciences (NIGMS) R01 GM115399 (to X.S.), R35 GM122548 (to T.B.K.), R01 HL054737 and R01 HL121387 (to S.R.C.), 5T32HL007731 (to H.H.), National Natural Science Foundation of China (Grant No. 31571107, 31871481 to Z.D.), and R35 GM122603 (to William F. DeGrado for support of Haifan Wu).

Notes

The authors declare no competing financial interest.

■ ACKNOWLEDGMENTS

W.M. gratefully acknowledges the use of the computing facility at Beckman Institute, University of Illinois. S.-Q. Z. is grateful to Dr. Meng-Long Feng for inspiration.

■ REFERENCES

(1) Tait, S. W. G.; Green, D. R. Mitochondrial regulation of cell death. *Cold Spring Harbor Perspect. Biol.* **2013**, *5* (9), a008706.

(2) Strasser, A.; Jost, P. J.; Nagata, S. The many roles of FAS receptor signaling in the immune system. *Immunity* **2009**, *30* (2), 180.

(3) Crawford, E. D.; Wells, J. A. Caspase substrates and cellular remodeling. *Annu. Rev. Biochem.* **2011**, *80*, 1055.

(4) Campbell, D. S.; Okamoto, H. Local caspase activation interacts with Slit-Robo signaling to restrict axonal arborization. *J. Cell Biol.* **2013**, *203* (4), 657.

(5) Yamaguchi, Y.; Shinotsuka, N.; Nonomura, K.; Takemoto, K.; Kuida, K.; Yosida, H.; Miura, M. Live imaging of apoptosis in a novel transgenic mouse highlights its role in neural tube closure. *J. Cell Biol.* **2011**, *195* (6), 1047.

(6) Takemoto, K.; Kuranaga, E.; Tonoki, A.; Nagai, T.; Miyawaki, A.; Miura, M. Local initiation of caspase activation in Drosophila salivary gland programmed cell death in vivo. *Proc. Natl. Acad. Sci. U. S. A.* **2007**, *104* (33), 13367.

DOI: 10.1021/jacs.8b13042
J. Am. Chem. Soc. 2019, 141, 4526−4530

(7) Takemoto, K.; Nagai, T.; Miyawaki, A.; Miura, M. Spatio-temporal activation of caspase revealed by indicator that is insensitive to environmental effects. *J. Cell Biol.* **2003**, *160* (2), 235.
(8) To, T.-L.; Schepis, A.; Ruiz-González, R.; Zhang, Q.; Yu, D.; Dong, Z.; Coughlin, S. R.; Shu, X. Rational design of a GFP-based fluorogenic caspase reporter for imaging apoptosis *in vivo*. *Cell Chemical Biology* **2016**, *23* (7), 875.
(9) To, T.-L.; Piggott, B. J.; Makhijani, K.; Yu, D.; Jan, Y.-N.; Shu, X. Rationally designed fluorogenic protease reporter visualizes spatio-temporal dynamics of apoptosis in vivo. *Proc. Natl. Acad. Sci. U. S. A.* **2015**, *112* (11), 3338.
(10) Ding, Y.; Li, J.; Enterina, J. R.; Shen, Y.; Zhang, I.; Tewson, P. H.; Mo, G. C. H.; Zhang, J.; Quinn, A. M.; Hughes, T. E.; Maysinger, D.; Alford, S. C.; Zhang, Y.; Campbell, R. E. Ratiometric biosensors based on dimerization-dependent fluorescent protein exchange. *Nat. Methods* **2015**, *12* (3), 195.
(11) (a) Do, K.; Boxer, S. G. GFP Variants with Alternative β-strands and Application as a Light-driven Protease Sensor: A Tale of Two Tails. *J. Am. Chem. Soc.* **2013**, *135* (28), 10226. (b) Deng, A.; Boxer, S. G. Structural Insight into the Photochemistry of Split Green Fluorescent Proteins: A Unique Role for a His-Tag. *J. Am. Chem. Soc.* **2018**, *140* (1), 375. (c) Do, K.; Boxer, S. G. Thermodynamics, Kinetics, and Photochemistry of β-Strand Association and Dissociation in a Split-GFP System. *J. Am. Chem. Soc.* **2018**, *140* (1), 375.
(12) Nicholls, S. B.; Chu, J.; Abbruzzese, G.; Tremblay, K. D.; Hardy, J. A. Mechanism of a genetically encoded dark-to-bright reporter for caspase activity. *J. Biol. Chem.* **2011**, *286* (28), 24977.
(13) Yu, D.; Baird, M. A.; Allen, J. R.; Howe, E. S.; Klassen, M. P.; Reade, A.; Makhijani, K.; Song, Y.; Liu, S.; Murthy, Z.; Zhang, S.-Q.; Weiner, O. D.; Kornberg, T. B.; Jan, Y.-N.; Davidson, M. W.; Shu, X. A naturally monomeric infrared fluorescent protein for protein labeling in vivo. *Nat. Methods* **2015**, *12* (8), 763.
(14) Yang, F.; Moss, L. G.; Phillips, G. N. The molecular structure of green fluorescent protein. *Nat. Biotechnol.* **1996**, *14* (10), 1246.
(15) Ormö, M.; Cubitt, A. B.; Kallio, K.; Gross, L. A.; Tsien, R. Y.; Remington, S. J. Crystal structure of the Aequorea victoria green fluorescent protein. *Science* **1996**, *273* (5280), 1392.
(16) Cabantous, S.; Terwilliger, T. C.; Waldo, G. S. Protein tagging and detection with engineered self-assembling fragments of green fluorescent protein. *Nat. Biotechnol.* **2005**, *23* (1), 102.
(17) Tsien, R. Y. Constructing and exploiting the fluorescent protein paintbox (Nobel Lecture). *Angew. Chem., Int. Ed.* **2009**, *48* (31), 5612.
(18) Tsien, R. Y. The green fluorescent protein. *Annu. Rev. Biochem.* **1998**, *67*, 509.
(19) Sniegowski, J. A. Base Catalysis of Chromophore Formation in Arg^{96} and Glu^{222} Variants of Green Fluorescent Protein. *J. Biol. Chem.* **2005**, *280* (28), 26248.
(20) Cabantous, S.; Nguyen, H. B.; Pédelacq, J.-D.; Koraïchi, F.; Chaudhary, A.; Ganguly, K.; Lockard, M. A.; Favre, G.; Terwilliger, T. C.; Waldo, G. S. A new protein-protein interaction sensor based on tripartite split-GFP association. *Sci. Rep.* **2013**, *3*, 2854.
(21) Zhang, Q.; Zheng, Y.-W.; Coughlin, S. R.; Shu, X. A rapid fluorogenic GPCR–β-arrestin interaction assay. *Protein Sci.* **2018**, *27* (4), 874.
(22) Sorrells, S.; Toruno, C.; Stewart, R. A.; Jette, C. Analysis of apoptosis in zebrafish embryos by whole-mount immunofluorescence to detect activated Caspase 3. *J. Visualized Exp.* **2013**, e51060,.
(23) Zhang, J.; Wang, X.; Cui, W.; Wang, W.; Zhang, H.; Liu, L.; Zhang, Z.; Li, Z.; Ying, G.; Zhang, N.; Li, B. Visualization of caspase-3-like activity in cells using a genetically encoded fluorescent biosensor activated by protein cleavage. *Nat. Commun.* **2013**, *4*, 2157.
(24) Tee, A. R.; Proud, C. G. Staurosporine inhibits phosphorylation of translational regulators linked to mTOR. *Cell Death Differ.* **2001**, *8* (8), 841.
(25) Albeck, J. G.; Burke, J. M.; Aldridge, B. B.; Zhang, M.; Lauffenburger, D. A.; Sorger, P. K. Quantitative analysis of pathways controlling extrinsic apoptosis in single cells. *Mol. Cell* **2008**, *30* (1), 11.
(26) Grunwald, D. J.; Eisen, J. S. Headwaters of the zebrafish – emergence of a new model vertebrate. *Nat. Rev. Genet.* **2002**, *3* (9), 717.
(27) Szymczak, A. L.; Workman, C. J.; Wang, Y.; Vignali, K. M.; Dilioglou, S.; Vanin, E. F.; Vignali, D. A. A. Correction of multi-gene deficiency in vivo using a single 'self-cleaving' 2A peptide-based retroviral vector. *Nat. Biotechnol.* **2004**, *22* (5), 589.
(28) Cole, L.; Ross, L. S. Apoptosis in the developing zebrafish embryo. *Dev. Biol.* **2001**, *240* (1), 123.
(29) Jiang, H.; Edgar, B. A. Intestinal stem cell function in Drosophila and mice. *Curr. Opin. Genet. Dev.* **2012**, *22* (4), 354.
(30) Apidianakis, Y.; Pitsouli, C.; Perrimon, N.; Rahme, L. Synergy between bacterial infection and genetic predisposition in intestinal dysplasia. *Proc. Natl. Acad. Sci. U. S. A.* **2009**, *106* (49), 20883.
(31) Liang, J.; Balachandra, S.; Ngo, S.; O'Brien, L. E. Feedback regulation of steady-state epithelial turnover and organ size. *Nature* **2017**, *548* (7669), 588.
(32) Okumura, T.; Takeda, K.; Taniguchi, K.; Adachi-Yamada, T. $\beta\nu$ integrin inhibits chronic and high level activation of JNK to repress senescence phenotypes in Drosophila adult midgut. *PLoS One* **2014**, *9* (2), No. e89387.
(33) Nguyen, H. B.; Hung, L. W.; Yeates, T. O.; Terwilliger, T. C.; Waldo, G. S. Split green fluorescent protein as a modular binding partner for protein crystallization. *Acta Crystallogr., Sect. D: Biol. Crystallogr.* **2013**, *69* (12), 2513.
(34) Fuchs, Y.; Steller, H. Programmed cell death in animal development and disease. *Cell* **2011**, *147* (4), 742.
(35) Jacobson, M. D.; Weil, M.; Raff, M. C. Programmed cell death in animal development. *Cell* **1997**, *88* (3), 347.
(36) Lopez-Otin, C.; Bond, J. S. Proteases: multifunctional enzymes in life and disease. *J. Biol. Chem.* **2008**, *283* (45), 30433.

DOI: 10.1021/jacs.8b13042
J. Am. Chem. Soc. 2019, 141, 4526–4530